

Proton Conductivity in $\text{BaTb}_{0.6}\text{In}_{0.4}\text{O}_{(2.8+y/2)}\text{H}_y$, a New Compound with the Simple Perovskite-like Structure

R. R. Arons*

Institut für Festkörperforschung, Forschungszentrum Jülich, D-52425 Jülich, Germany

Abstract

The water uptake in the new perovskite-like compound $\text{BaTb}_{0.6}\text{In}_{0.4}\text{O}_{2.8}$, further called BTI40, has been measured in situ by thermal gravimetric analysis (TGA) at different temperatures and water vapour pressures. For the standard enthalpy and entropy of solution the following values were deduced:

$$\Delta H^0 = (-0.79 \pm 0.02) \text{ eV}$$

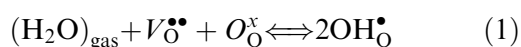
and

$$\Delta S^0 = (-1.3 \pm 0.1) \times 10^{-3} \text{ eV/K}$$

The grain interior electrical conductivity, σ_{gi} , of a BTI40 pellet has been measured in the dry state and for proton concentrations of 2.3, 3.3 and 3.7% in the wet state by impedance spectroscopy. In the range from 100 to 450 °C, in which the proton concentration is frozen in, σ_{gi} increases linearly with the proton concentration, being about a factor of 50 larger than that in the dry state. The activation energy of the proton conduction is found to be $(0.65 \pm 0.01) \text{ eV}$. © 1999 Elsevier Science Limited. All rights reserved

Keywords: thermogravimetry, impedance, ionic conductivity-proton, perovskites.

Some oxides with the perovskite-like structure, ABO_3 , are well known to become high-temperature proton conductors (HTPC) upon acceptor-doping.¹ Typical examples are BaCeO_3 and SrCeO_3 doped with trivalent Y- or Yb-ions at the Ce^{4+} -sites. In order to retain charge neutrality upon doping, vacancies at the O-sites are introduced. By subsequent annealing in a humid atmosphere protons are incorporated by the dissociative absorption of water according to the reaction:



where $V_{\text{O}}^{\bullet\bullet}$ represents the double positively charged vacancies on the O-sites and $\text{OH}_{\text{O}}^{\bullet}$ the positively charged protonic defects. Recently we have shown that BaTbO_3 can be acceptor-doped with large amounts of indium (further called BTI).² Up to atomic ratios of $x = \text{In}/(\text{In} + \text{Tb}) = 0.47$ the In^{3+} - and Tb^{4+} -ions occupy the B-sites of the perovskite oxide at random and the total amount of $V_{\text{O}}^{\bullet\bullet}$ expected from the In-concentration is completely filled up by annealing in a humid Ar/O_2 (80/20) mixture with $p_{\text{H}_2\text{O}} = 100 \text{ hPa}$, and slowly cooling in about 16 h from $T = 300$ to 150 °C ($1 \text{ hPa} = 10^2 \text{ Pa} = 1 \text{ mbar}$). Accordingly, for BTI40 ($x = 0.40$) the chemical formula of the compound is given by $\text{BaTb}_{0.6}\text{In}_{0.4}\text{O}_{(2.8+y/2)}\text{H}_y$, in which $y = 0$ and $y = 0.4$ represent the fully 'dry' and fully 'wet' states, respectively. In view of the huge amount of protons that can be incorporated, BTI was suggested as a new possible candidate for a HTPC.² In the present work we have studied the in-situ proton incorporation and the equilibrium $[\text{OH}_{\text{O}}^{\bullet}]$ -concentrations in BTI40 by thermal gravimetric analysis (TGA). The experiments were carried out in a commercial thermobalance (Netzsch TG 439) modified for wet atmospheres, as described elsewhere.³ The experiments were performed in the isothermic mode and at each temperature ($300 \leq T [\text{°C}] \leq 800$) a series of four partial water vapour pressures $p_{\text{H}_2\text{O}} = 5, 10, 20$ and 40 hPa was applied. In addition first ac-impedance spectroscopy experiments are presented.

The expression for the equilibrium constant K_3 for the reaction in eqn (1) is given by:

$$K_3 = \frac{[\text{OH}_{\text{O}}^{\bullet}]^2}{(p_{\text{H}_2\text{O}}/p^0)[\text{O}_{\text{O}}^x][V_{\text{O}}^{\bullet\bullet}]} \quad (2)$$

where $kT \ln K_3 = T\Delta S^0 - \Delta H^0$; ΔH^0 and ΔS^0 are the standard enthalpy and entropy of solution, respectively; p^0 represents the standard pressure of 10^5 Pa (1 bar). The concentrations in eqn (2) are considered per Ba atom in the formula unit

*Fax: +49-2461-61-8207; e-mail: r.arons@fz-juelich.de

BaTbO₃ (in which no defects are present); accordingly in BaTb_{0.6}In_{0.4}O_(2.8+y/2)H_y, it holds that $[\text{OH}_o^\bullet] = y$.

From the condition of charge neutrality:

$$2[V_{\text{O}}^{\bullet\bullet}] + [\text{OH}_o^\bullet] - [\text{In}_{\text{Tb}}'] + [\text{In}_{\text{Ba}}^\bullet] = 0$$

and taking into account that in BTI the maximum proton concentration $[\text{OH}_o^\bullet]_{\text{max}}$ equals the total In-concentration, it follows that $[\text{In}_{\text{Ba}}^\bullet] = 0$, so that:

$$2[V_{\text{O}}^{\bullet\bullet}] = [\text{OH}_o^\bullet]_{\text{max}} - [\text{OH}_o^\bullet] \quad (3)$$

From eqn (3) and the condition of site restriction, given by:

$$[O_o^x] + [V_{\text{O}}^{\bullet\bullet}] + [\text{OH}_o^\bullet] = 3$$

the following expression for $[O_o^x]$ is obtained:

$$[O_o^x] = \left\{ 3 - \frac{1}{2} [\text{OH}_o^\bullet]_{\text{max}} \right\} - \frac{1}{2} [\text{OH}_o^\bullet] \quad (4)$$

In the cerates and zirconates usually this change of $[O_o^x]$ as a function of $[\text{OH}_o^\bullet]$ is neglected in view of the low solubility of the $[\text{OH}_o^\bullet]$ -defects of only a few per cent. However, in BTI40, $[O_o^x]$ decreases from 2.8 for $y = [\text{OH}_o^\bullet] = 0$ to 2.6 for $y = [\text{OH}_o^\bullet] = [\text{OH}_o^\bullet]_{\text{max}} = 0.4$, so that this variation of $[O_o^x]$ as a function of $[\text{OH}_o^\bullet]$ must be taken into account. Substituting eqn (3) and eqn (4) into eqn (2), it follows that the value of K_3 only depends on $p_{\text{H}_2\text{O}}$, $[\text{OH}_o^\bullet]$ and $[\text{OH}_o^\bullet]_{\text{max}}$. Accordingly, when the value of $[\text{OH}_o^\bullet]_{\text{max}}$ is known, K_3 is readily calculated for each $[\text{OH}_o^\bullet]$ content. A fully charged BTI40 sample, dried in the present TGA-apparatus, showed that $[\text{OH}_o^\bullet]_{\text{max}} = 0.41$. This suggests that the indium concentration $x = 0.41$ in the present material, in agreement with the lower Néel temperature of $T_N = 13.5$ K instead of 16 K observed for BTI40 in Ref.2.

In Fig. 1, we present the proton content $[\text{OH}_o^\bullet]$ as a function of water vapour pressure for various temperatures. The highest equilibrium concentration of $[\text{OH}_o^\bullet] = 0.183$ obtained at the lowest temperature of $T = 300$ °C and highest pressure of 40 hPa is still far away from the maximum concentration of 0.41 obtained by using a pressure of 100 hPa and slowly cooling from $T = 300$ to 150 °C. In Fig. 2 we have plotted the corresponding K_3 values as a function of the reciprocal temperature for the four water vapour pressures. In view of the scattering of the data observed at 800 °C, probably due to the low $[\text{OH}_o^\bullet]$ -solubility at this temperature, we have skipped the latter data in the evalua-

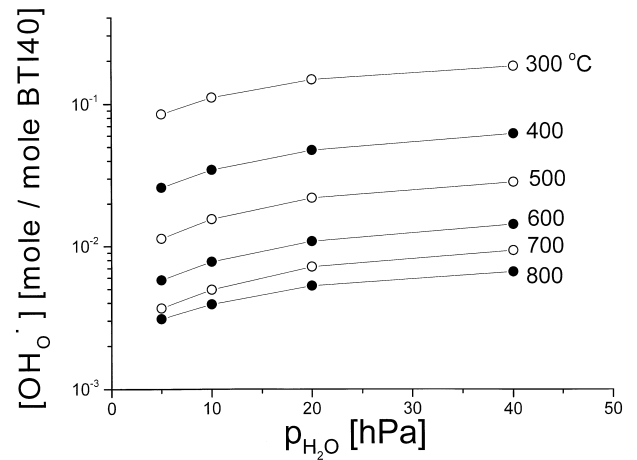


Fig. 1. Equilibrium $[\text{OH}_o^\bullet]$ -concentration = y in BaTb_{0.6}In_{0.4}O_(2.8+y/2)H_y as a function of water vapour pressure for various temperatures (1 hPa = 10² Pa = 1 mbar). Because of clearness of the data presentation, a logarithmic scale has been chosen.

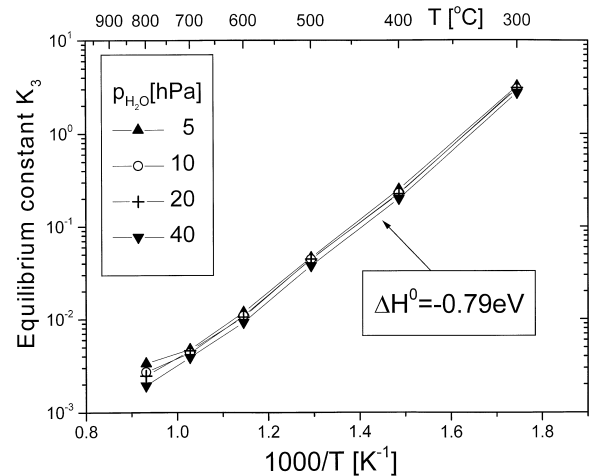


Fig. 2. Equilibrium constant K_3 for the $[\text{OH}_o^\bullet]$ -solubility in BTI40 versus reciprocal temperature, as obtained from four different water vapour pressures (1 hPa = 1 mbar).

tion. For the other temperatures the data sets at the four different vapour pressures show excellent agreement. From the slope of each data set the same enthalpy of solution $\Delta H^0 = (-0.79 \pm 0.02)$ eV is deduced, while for the entropy of solution an average value $\Delta S^0 = (-1.3 \pm 0.1) \times 10^{-3}$ eV/K is obtained. These values are comparable to those observed in BaSn_{0.5}In_{0.5}O_{2.75}⁴ and BaCa_{1.18}Nb_{1.82}O_{2.91} (BCN18).³ On the other hand, in BaCe_(1-x)Y_xO_(3-x/2), ΔH^0 was recently found to vary from -1.2 to -1.8 eV in the range from $x = 0.02$ to 0.2, suggesting that the solubility in the latter material is much higher.⁵

Now we will discuss the ac impedance spectroscopy of a BTI40 pellet with 0.91 cm diameter and 0.16 cm thickness. The measurements were performed at rising temperatures between 50 and 600 °C in an environment of a flowing dry Ar/O₂ (80/20) mixture. After sintering at 1500 °C, both sides of the pellet were polished and covered with

porous Pt paint (ESL type 5542) electrodes which were fixed by heating at 980°C . Two different methods were applied to obtain a ‘dry’ pellet for the impedance spectroscopy: in one case the pellet was annealed in vacuum (10^{-4} Pa) at 530°C ; in the other a flowing dry Ar/O_2 (80/20) mixture at 700°C was used. After the impedance measurement the pellet was charged for about 60 h at various temperatures between 600 and 450°C in a wet 80 $\text{Ar}/20$ O_2 mixture with $p_{\text{H}_2\text{O}} = 100$ hPa. Since the weight of the pellet was found to be unchanged before and after the impedance measurements, it follows that the amount of protons incorporated are frozen in during the conductivity measurements. The impedance spectra were recorded at frequencies, f , between 100 mHz and 2 MHz, using a Solartron SI1260 impedance analyzer.

Usually impedance spectra of ceramic samples are analyzed within the framework of the ‘brick layer’ model.⁶ This model leads to an equivalent circuit in which the grain interior is characterized by a resistance R_{gi} and the geometrical capacitance C_V , and the grain boundaries by R_{gb} and C_{gb} , respectively. The corresponding impedance spectrum ($-Z''$ versus Z') consists of two semi-arcs, in which the first one at lower resistance values (higher frequencies) is ascribed to the grain interior and the other one to the grain boundaries. Figure 3 shows a typical $-Z''$ versus Z' spectrum of BTI40 in the ‘dry’ state at 300°C (open circles). Only one half circle is observed, which is ascribed to the grain interior in the following. From the condition $2\pi fRC = 1$ at the maximum of the semi-arc, the capacitance is calculated to be $C = 47$ pF, a value typical of the grain interior. By comparing the known geometrical capacitance and the value measured for the bulk, a value of $\epsilon_r \approx 140$ for the relative static permittivity of BTI40 is derived.

The insert of Fig. 3 shows the high-frequency part of the impedance spectrum on an enlarged scale. It is seen that the resistance of the ‘dry’ sample at 300°C is strongly reduced by the incorporation of the 3.7% protons (full triangles). As for the dry sample, from the values of f and Z' at the maximum of $-Z''$, the capacitance of the wet sample is calculated to be $C = 40$ pF, comparable with the value obtained before for the dry sample. Thus also the semi-arc obtained for the humid sample must be ascribed to the grain interior and the relative static permittivities in the two different states are roughly the same. The values of R_{gi} at 300°C are obtained from the diameter of the half-circles fitted to the data of Fig. 3. From this, the conductivity is calculated from the relation $\sigma_{gi} = d/AR_{gi}$, where A denotes the electrode area and d the sample thickness. In Fig. 4, σ_{gi} is plotted versus the reciprocal temperature for various

$[\text{OH}_o^\bullet]$ -contents. The dry sample shows a curvature in the $\sigma_{gi}T$ versus $1/T$ plot. This result does not depend on whether the sample has been dried in vacuum or in a dry Ar/O_2 (80/20) mixture before the experiment. Taking into account that also the conductivity is obtained in the latter atmosphere, we believe that this increase of the activation enthalpy at high temperatures is not caused by an exchange of the oxygen in the sample with the gas phase at sufficiently high temperatures of measurement but is an intrinsic effect of BTI40 in the dry state. From the high- and low-temperature slopes of the $\sigma_{gi}T$ versus $1/T$ curve, activation enthalpies $E_a \approx 1.1$ eV and $E_a \approx 0.48$ eV, respectively, are obtained. This suggests that two different mechanisms are involved in the conductivity of the ‘dry’ BTI40 sample.

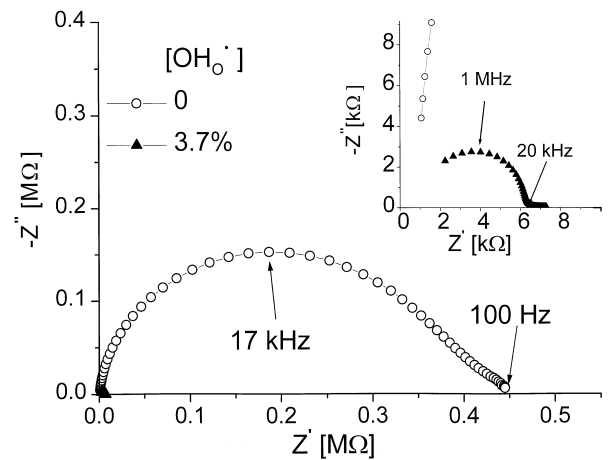


Fig. 3. Impedance spectra of BTI40 at 300°C in the dry and wet states, showing the strong reduction of the resistance R_{gi} due to the 3.7% protons. The insert shows the high-frequency part of the spectra on an enlarged scale. The frequency values, f , at the maximum $-Z''$ -values and the low frequency sides of the semi-arcs are indicated.

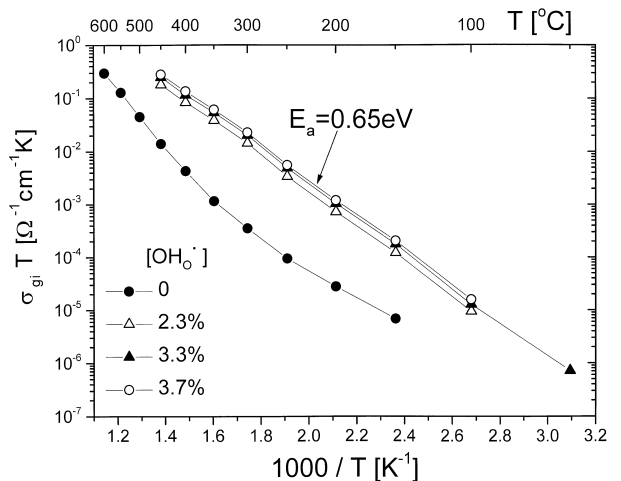


Fig. 4. Temperature dependence of the grain interior conductivity of BTI40 in the dry and wet states. The samples were measured at rising temperatures in a dry Ar/O_2 (80/20) environment. The proton concentrations indicated are obtained from the weight increase of the sample and remain unchanged during the experiment.

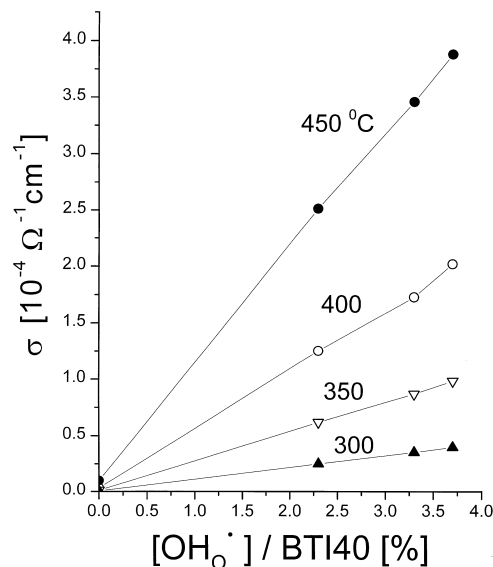


Fig. 5. Grain interior conductivity of BTI40 as a function of the total proton concentration frozen in for various temperatures.

Figure 4 also presents the temperature dependence of the conductivity for the three proton concentrations up to 450 °C. As mentioned above, up to this temperature the amount of protons incorporated by the charging treatment remains frozen in during the conductivity measurements. The conductivity of BTI40 in the wet state is seen to be increased by a factor of 20 to 60 in the range from 450 to 250 °C compared with that in the dry state. The three wet samples show identical slopes with $E_a = (0.65 \pm 0.01) \text{ eV}$. The $[\text{OH}_O^\bullet]$ -concentration dependence of the conductivity becomes better visible from a linear scale for σ_{gi} , as follows from Fig. 5. This figure shows the conductivity of BTI40 as a function of the $[\text{OH}_O^\bullet]$ -concentration in the range from 300 to 450 °C. While the values of σ_{gi} in

the dry state appear around the origin, σ_{gi} of the three samples in the wet state is seen to increase linearly with the proton concentration frozen in. This suggests that it is the proton conduction which is responsible for the increase of the total conductivity measured.

Investigations of the influence of the indium concentration on the proton solubility and conduction in BTI are in progress.

Acknowledgements

Mr J. Friedrich is gratefully acknowledged for performing the TGA measurements. The author is much indebted to Dr H.G. Bohn for invaluable discussions during this work.

References

1. Iwahara, H., High temperature protonic conductors and their applications. In *Solid State Ionics*, ed. M. Balkanski, T. Takahashi, H. L. Tuller. Elsevier, Amsterdam, 1992, p. 575–586.
2. Arons, R. R., Magnetic studies of the Ba-Tb-In-oxide, a new proton conductor with the simple perovskite-like structure. *J. Mag. Magn. Materials*, 1998, **177–181**, 869–870.
3. Krug, F. and Schober, T., The high-temperature proton conductors $\text{Ba}_3(\text{Ca}_{1.18}\text{Nb}_{1.82})\text{O}_{9.8}$. *Solid State Ionics*, 1996, **92**, 297–302.
4. Schober, T., Protonic conduction in $\text{BaI}_{0.5}\text{Sn}_{0.5}\text{O}_{2.75}$. *Solid State Ionics*, 1998, **109**, 1–11.
5. Kreuer, K. D., Münch, W., Ise, M., He, T., Fuchs, A., Traub, U. and Maier, J., Defect Interactions in proton conducting perovskite-type oxides. *Ber. Bunsenges. Phys. Chem.*, 1997, **101**, 1344–1350.
6. Christie, G. M. and van Berkel, F. P. F., Microstructure-ionic conductivity relationships in ceria-gadolinia electrolytes. *Solid State Ionics*, 1996, **83**, 17–27.